Calculation of Left Ventricular Volume from 3D Echocardiography: a Comparison of Three Image Analysis Techniques

J Wild[1], AJ Sims[1,2], J Pemberton[3], T Irvine[4], A Kenny[3], A Murray[1,2]

[1]University of Newcastle, Newcastle upon Tyne, UK
[2]Regional Medical Physics Department, Freeman Hospital, Newcastle upon Tyne, UK
[3]Department of Cardiology, Freeman Hospital, Newcastle upon Tyne, UK
[4]Department of Cardiology, Royal Victoria Infirmary, Newcastle upon Tyne, UK

Abstract

Left ventricular volume is an important clinical indicator for the diagnosis and the monitoring of treatment of many heart diseases. Automated quantification using echocardiography is challenging due to inherent image artefacts. In this paper, three different methods for calculating left ventricular volume were compared.

3D images of the left ventricle (LV) were reconstructed from rotationally acquired B-mode images for six patients at end-diastole and end-systole. By manual selection of the LV long-axis centre line, virtual, contiguous perpendicular short-axis images could be extracted. The LV wall was then detected by using (a) circle fitting, (b) smoothing between circles, and (c) greedy snake.

Results of this study showed that there was no significant difference between chamber volume estimated by all three techniques.

1. Introduction

Left ventricular volume is important in clinical assessment because abnormal volume or shape is indicative of abnormal function or pathology [1]. SPECT (conventional single-photon emission computed tomography) is often used in clinical practice but is costly and ionising. Ultrasound, in comparison, does not expose the patient to a radiation dose, but is subject to image noise and makes automated analysis non-trivial.

Traditionally, two-dimensional images have been used for volume calculation, but this involves making geometric assumptions about the shape of the heart [2]. To calculate a 3D quantity accurately a 3D representation is needed. Schroder *et al* [3] and Abdullah *et al* [4] have shown that 3D echocardiography is superior to 2D echocardiography for LV volume quantification in digital models and small piglet hearts respectively. Several authors have looked at reconstruction of 3D ultrasound images from a sequence of 2D images. Freehand ultrasound was employed by Barry *et al* [5] and Nguyen *et al* [6] used a rotating probe to image a dynamic cardiac phantom and found that calculated volumes were in agreement with those measured from gated SPECT.

The aims of this study were to investigate the repeatability and differences of three methods for calculating LV volume from reconstructed 3D trans-oesophageal echocardiography.

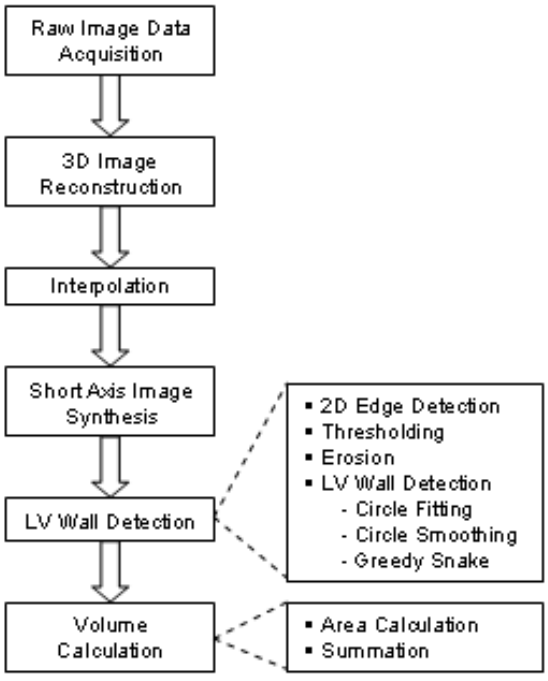

Figure 1. Flowchart showing the steps of the method from initial data collection to volume output.

2. Methods

2.1. Image acquisition

An ATL HDI 5000 ultrasound system with a 7MHz rotating trans-oesophageal probe (MPT 7-4) was used to image six patients with impaired LV function. Ventilation was suspended during two sequential scans for each patient. A fixed number of frames, dependent on the patient's heart rate (range 12-18), were captured at equal time intervals during each cardiac cycle. Each frame comprised 128 A-mode scan lines with a depth of 512 pixels spaced equally over a 90° arc. The transducer probe was rotated by 6° after each cycle a total of 30 times to ensure 180° coverage of the left ventricle. Two frames from each study were visually identified based on cavity area for end-diastole (ED) and end-systole (ES). The time difference between the start of the first scan and the start of the second scan ranged from approximately 2 minutes to 5 minutes.

2.2. 3D reconstruction

3D images were created by transforming the 2D ultrasound polar co-ordinates of each pixel into 3D Cartesian co-ordinates and assigning the intensity of the pixel to the target voxel. This produced sparsely populated 3D images. In a previous paper [7], differences between algorithms for spatial interpolation of 3D echocardiography images were studied. A 1D linear interpolation method was applied to all unassigned pixels that lay within the ultrasound conical volume in two stages: firstly in the original planes of acquisition where pixels were filled along arcs of equal distance from the probe origin, and secondly in perpendicular planes to the beam axis along arcs of equal radial distance.

2.3. Volume calculation

Manual selection of a proximal point inferior to the mitral valve and another superior to the apex were chosen to provide an approximate LV centre line. A series of perpendicular contiguous planes along 80% of the LV centre line from the apex were extracted. The remaining 20% were omitted to avoid difficulties with the mitral valve leaflets in the segmentation process. The LV wall was then found for each plane and the volume calculated by summation of the LV areas multiplied by the known voxel volume in ml. Figure 1 shows the various steps of the process from initial data collection to volume calculation.

2.4. LV wall detection

Three different methods were used to detect the LV wall:-

Circle: The LV wall was modelled by the largest circle which included the LV centre line and did not include any muscle tissue [8]. This was achieved by subjecting each 2D image to edge detection via a 7×7 truncated pyramid edge detector [9] followed by thresholding and binary erosion to produce a binary edge map upon which a circle could be fitted.

Circle smoothing: Erroneous circles were rejected in three steps: i) circles with a radius larger than the normal upper limit of LV size (6cm for ED and 4cm for ES) were rejected; ii) circles were rejected if the radii and centre differences were greater than a pre-defined value; iii) values for the radii and centre of rejected circles were linearly interpolated from nearest accepted circles.

Greedy snake: A greedy snake as defined by Williams and Shah [10] was implemented using the smoothed circles as initialisation for the starting position of the snake. Along with curvature and continuity constraints the snake was influenced by an edge map. The edge map was created by applying the same edge operator as in the circle algorithm on a Gaussian smoothed image. With each snake iteration the amount of smoothing was reduced. Once the snake had reached the optimum position a piecewise Bezier curve [11] was fitted to the snake points.

2.5. Method of comparision

Repeatability of each LV wall detection was measured by the method of Bland and Altman [12]. LV volumes for all six patients for each phase and scan were calculated. The volume differences between original and repeat scans were calculated for each method, in addition to the between-method differences.

3. Results

Figure 2 shows three reconstructed LV long-axis images for patient 1 at ED with the detected LV wall for the different methods shown by the white dots. Visually, the examples show that each method found a different position for the LV wall. Figure 3 shows two example reconstructed LV short-axis images taken from the same patient with the circle and snake superimposed. The snake more accurately followed the LV border than the circle.

Table 1 shows that for each method and phase the confidence interval included zero, indicating no significant difference. The circle method has the largest variability for both phases with the smoothed circle and snake method having similar values.

(a)

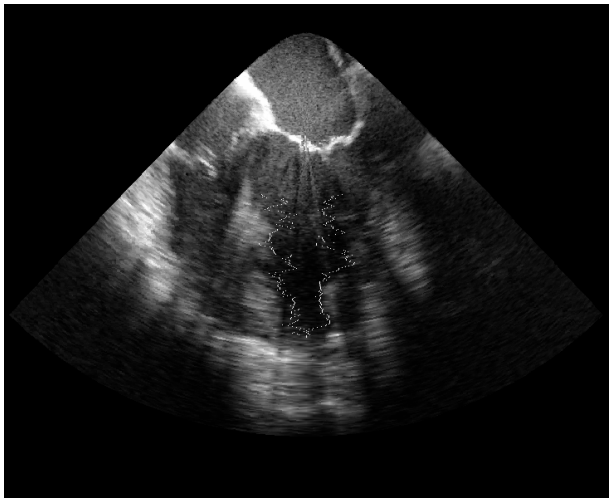

(b)

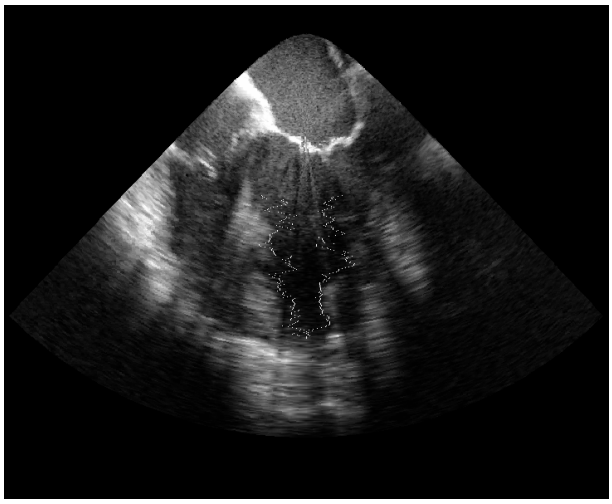

(c)

Figure 2. Reconstructed long-axis view for patient 1 at ED with the white dots being the projections of the, (a) circles (b) smoothed circles (c) snake, method used to detect the LV wall.

Table 1. Overall volume differences between two scans (original and repeat) for each phase and LV volume method for six patients. Differences are original - repeat.

End Diastole	Bias (ml)	95% C.I. of bias	sd (ml)
Circle	19	(-21 , 60)	38
Smoothed Circle	3	(-6 , 12)	9
Snake	2	(-9 , 12)	10
End Systole	**Bias (ml)**	**95% C.I. of bias**	**sd (ml)**
Circle	-1	(-11 , 10)	10
Smoothed Circle	-4	(-11 , 3)	6
Snake	-4	(-11 , 4)	7

Table 2. Mean ED and ES volumes (ml) over two scans are shown along with between phase volume.

Method	Patient	Mean ED Volume (ml)	Mean ES Volume (ml)	Between Phase Volume (ml)
Circle	1	23	13	10
	2	48	28	20
	3	46	20	26
	4	65	32	32
	5	24	10	14
	6	47	31	16
Smoothed Circle	1	43	27	16
	2	48	24	24
	3	38	20	17
	4	22	22	0
	5	24	10	15
	6	49	33	16
Snake	1	23	14	9
	2	51	24	26
	3	39	22	17
	4	22	22	0
	5	25	11	14
	6	52	35	17

Original and repeat volumes were averaged to give a mean value for each combination of LV wall detection method and phase (table 2). The between phase volume was calculated from the ED and ES values. The between phase volume for patient 4 for the smoothed circle and snake methods was close to zero. This was due to the poor quality of the images.

A Bland and Altman analysis applied to the volume differences between the three methods showed no significant difference (table 3).

4. Discussion

Reconstructing 3D images allowed virtual image planes to be extracted. For LV volume calculation three different LV wall detection methods were applied to virtual short-axis images, and the areas summed to give a volume.

Table 1 shows that there is no significant bias between

Table 3. Bland and Altman analysis of overall volume differences between three methods of LV wall detection.

Methods	Phase	Bias (ml)	95% CI of bias (ml)
circle–smoothed	ED	4	(-17, 26)
	ES	0	(-9, 8)
circle–snake	ED	7	(-13, 26)
	ES	1	(-5, 6)
smoothed–snake	ED	2	(-7, 11)
	ES	1	(-5, 7)

repeats for all methods. From the standard deviations, the circle method was the most variable especially at ED. It had a standard deviation of 38ml compared to 9ml and 10ml for the smoothed circles and snake methods respectively. This was due to the circles being defined by using just three edge points. Small shifts in those points caused significant changes to circle definitions. This was more pronounced for larger circles. Using information from proximal and distal circles helped to reject inaccurate circles (figure 2 (a), (b)). All three methods struggled when there was significant signal attenuation and shadowing.

Qualitatively, modelling the LV wall with a circle gave a fair approximation, but in many cases the snake was able to improve upon this (figure 3). There were occasions when the snake wrongly settled on false edges due to noise and shadowing. In future studies it is hoped that by improving the snake algorithm this problem could be reduced. Other plans for future investigation include 3D edge detectors to further make use of the 3D information present, and to also validate the automated volumes by an independent method.

The ventricular volumes were smaller than would have been expected if the complete LV volume had been estimated, but in this preliminary study only the ventricular apex volume was included.

In this study, three different methods have been investigated. All have been shown to have no significant difference between the volumes calculated by them.

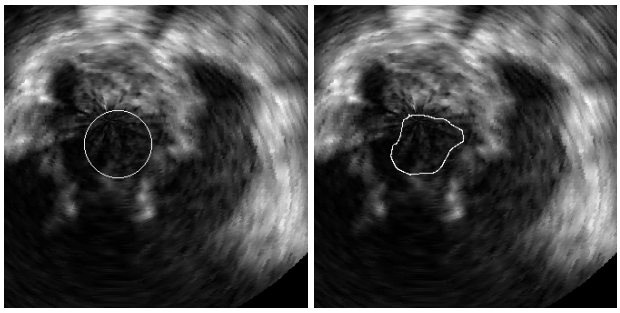

(a) (b)

Figure 3. Section of reconstructed short-axis view for patient 1 at ED approximately midway along LV centre line with (a) circle superimposed (b) snake superimposed

References

[1] Sutton P. Measurements in Cardiology. New York, USA: Parthenon Publishing Group, 1999.

[2] Quinones M, Waggoner A, Reduto L, Nelson J, Young J, Winters W, Ribeiro L, Miller R. A new simplified method for determining ejection fraction with two-dimensional echocardiography. Circulation 1981;64:744–753.

[3] Schroder K, Sapin P, King D, Smith M, DeMaria A. Three-dimensional echocardiographic volume computation: In vitro comparison to standard two-dimensional echocardiography. J Am Soc Echocardiogr 1993;6:467–475.

[4] Abdullah M, Maeno Y, Bigras J, McCrindle B, Smallhorn J, Boutin C. Superiority of 3-dimensional versus 2-dimensional echocardiography for left ventricular volume assessment in small piglet hearts. J Am Soc Echocardiogr 2000;13:918–923.

[5] Barry C, Allott C, John N, MEllor P, Arundel D, Thomson D, Waterton J. Three-dimensional freehand ultrasound: image reconstruction and volume analysis. Ultrasound Med Biol 1997;23:1209–1224.

[6] Nguyen L, Leger C, Debrun D, Therain F, Visser F, Sokole E. Validation of a volumic reconstruction in 4-d echocardiography and gated spect using a dynamic cardiac phantom. Ultrasound Med Biol 2003;29:1151–1160.

[7] Sims A, Wild J, Pemberton J, Irvine T, Kenny A, Murray A. Differences between algorithms for spatial interpolation of 3d echocardiography images. Computers in Cardiology 2003;30:185–188.

[8] Sims A, Pemberton J, Irvine T, Kenny A, Murray A. Mapping the left ventricular cavity by analysis of images reconstructed from 3d trans-oesophageal echocardiography. Computers in Cardiology 2002;29:351–354.

[9] Pratt W. Digital Image Processing. Second edition. New York, USA: John Wiley & Sons Inc, 1991.

[10] Williams D, Shah M. A fast algorithm for active contours and curvature estimation. Comput Vision Graph 1992; 55:14–26.

[11] Hearn D. Computer Graphics, C Version. New Jersey, USA: Prentice Hall, 1997.

[12] Bland J, Altman D. Statistical methods for assessing agreement between two methods of clinical measurement. Lancet 1986;1:307–310.

Address for correspondence:

Joanne Wild
University of Newcastle upon Tyne
Medical Physics, Freeman Hosptial
Newcastle upon Tyne, UK
joanne.wild@nuth.northy.nhs.uk